Computational Model Development for Performance Analysis of Anode Baking Furnace

Tushar Thorat[1], Mukul Modak[2], Vibhav Upadhyay[3], Sheetal Gupta[4], Kiran Bhor[5], Amit Gupta[6]and Jagannath Nayak[7]

1. Scientist
4. Scientist
5. Senior Scientist
6. Lead Scientist

Aditya Birla Science & Technology Company, Taloja MIDC Panvel, Maharashtra, India

2. Manager
3. Assistant Vice President
7. President

Hindalco Industries Ltd., Reduction Plant, Renukoot, Uttar Pradesh, India

Corresponding author: tushar.thorat@adityabirla.com

Abstract

Hindalco's Renukoot smelter uses prebaked carbon anodes in Aluminium reduction cells. In past one year, pot room has reported several occurrences of anode cracking and carbon dusting. Quality control lab have frequently reported high electrical resistivity (> 56 μΩ-m) and low crystalline length (< 30 Å) in baked anode samples. These shortcomings in anode quality can be attributed to raw material quality, recipe, green anode process, and baking process. Based on plant data analysis and process study, baking process was identified as the major influencing factor. To find out root causes behind the sub-standard baking, performance analysis of Anode Baking Furnace (ABF) was carried out. A 3D CFD model was developed for analysing flue gas distribution and anode temperature profile during baking cycle. Thermal mapping experiment was performed to measure anode temperature at various heights in four different pits of a section. Model was calibrated and computed results were validated against the measured anode temperatures. Samples of anodes from these four pits were collected and analysed in laboratory. Velocity distribution of flue gas was analysed with CFD model. It was observed that, due to low velocity of flue gas in top region of flue wall, cold spots are created. Non-uniform gas flow distribution and heat losses from packing coke surface results in lower baking temperature and residence time of anodes located in top layer. Hence, quality parameters (ER, Lc, RD etc.) of these anodes were found below acceptable limits

Keywords: Anode baking furnace, CFD model, Thermal mapping, Performance analysis, Anode quality.

1. Introduction

Hindalco's Renukoot smelter operates with low amperage potlines which uses prebaked carbon blocks as anodes. Daily requirement of these anodes is fulfilled by one paste plant, three anode baking furnaces and one anode rodding shop. Having a good quality anode is important to ensure efficient and smooth operation in smelters. Properly compacted and baked anodes exhibit maximum service life, low anode voltage drop and ability to work at higher current densities. In past one-year, increased carbon dust and incidents of vertical anode cracking was reported by pot-room operation team. Anode quality data trends for this period show consistently high values of electrical resistivity (ER) and less than desired crystalline length (Lc).

Detailed studies have been performed to identify causes behind carbon dusting and anode cracking [2]. Poor anode baking, high Sodium and Vanadium content and insufficient anode

covering are known as the most dominant causes behind carbon dusting due to wear of carbon anodes [1,2]. Vertical anode cracking mainly results due to: (i) excessive internal stress generated due to high differential gradient between thermal expansion coefficient between yoke and carbon block, (ii) High heating rate during baking [2]. High heating rate during baking can be correlated with placement of anodes near the flue wall or bulged structure of flue-wall. High ER of carbon anodes can be attributed to poor Calcined Petroleum (CP) coke quality, under or over-pitching, improper compaction, and poor graphitization of green anodes during baking. Baking temperature and soaking time of anodes play critical role in graphitization and hence, in deciding final Lc of baked anodes [3].

In current study, chemical composition and physical properties of raw material coke were critically examined and found in desired range. Historical trends for significant green anode process parameters like granulometry of raw coke, mixing temperature, vibration time, vacuum, die pressure and green anode density were also found in desired limits. However, based on poor Lc trend, baking process was identified as the most dominating cause. To analyse the performance of anode baking furnace (ABF) in detail, a computational model was developed in the present study. ABF under study is a horizontal ring open top furnace. It is comprised of 2 fires. Each fire is divided into 13 sections. Green anodes are loaded in loading section. Loading section is followed by preheating 1, preheating 2 and preheating 3 sections. Preheating sections are followed by 3 heating or burner bridge sections. Heating sections are followed by 5 cooling sections. Last section is used for unpacking of anodes. Each section consists of 9 pits and 10 flue walls. Each pit is loaded with 77 anodes, 11 layers and 7 columns. Schematic of the furnace can be seen in Figure 1.

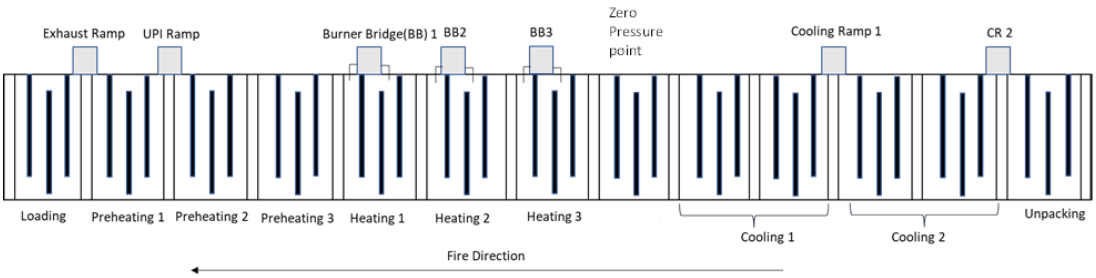

Figure 1. Process flow diagram of anode baking furnace under study.

Description of functional and physical features of these 14 sections are tabulated in Table 1.

Table 1. Summary of ABF operation.

Section	Flue inlet temperature	Flue exit temperature	Anode inlet temperature	Anode final temperature	Equipment	Physical Phenomena
Loading			50	90		Sensible heating of anodes, flue wall bricks and packing coke
Preheat 1	700	400	90	280	Exhaust Ramp	
Preheat 2	900	700	280	480	UPI (Under pressure instrument) Ramp	Pitch Volatile release from anodes and volatile combustion in flue gas, sensible heating of solids
Preheat 3	950	900	480	720		

Section	Flue inlet temperature	Flue exit temperature	Anode inlet temperature	Anode final temperature	Equipment	Physical Phenomena
Heating 1	1100	950	720	960	Burner Bridge 1	Fuel combustion on flue side, Graphitization of anode on pit side
Heating 2	1180	1100	960	1030	Burner Bridge 2	
Heating 3	1180	1180	1030	1080	Burner Bridge 3	
Cooling 1		1180	1080	720	Cooling Ramp 1	Preheating of hot air, sensible cooling of anodes, bricks and packing coke
Cooling 2	50		720	490	Cooling Ramp 2	

A computational model is developed for predicting gas flow distribution & temperature inside flue wall as well as baked anode temperature profile inside pit of the furnace. Anode temperature was measured at top, middle and bottom layer of anode inside the pit. Measured data was used to validate the computational results. To study the impact of baking temperature variation across the layers of anodes in a pit, samples from various heights were collected and characterized in laboratory. This work is discussed in upcoming sections of paper.

2. Computational Model of ABF

A 3-dimensional transient model was developed using ANSYS Fluent commercial code. To reduce computational time, the geometry or computational domain considered in model include only half section of anodes in pit, packing coke, and one flue wall adjacent to the pit. To model heat loss from the bottom of furnace, a representative concrete tub half section is also included in geometry. A pictorial representation of the computational domain is given in Figure 2. Same geometry was used to simulate preheating, heating, and cooling sections in ABF. Governing equations and boundary conditions used for these simulations are explained below.

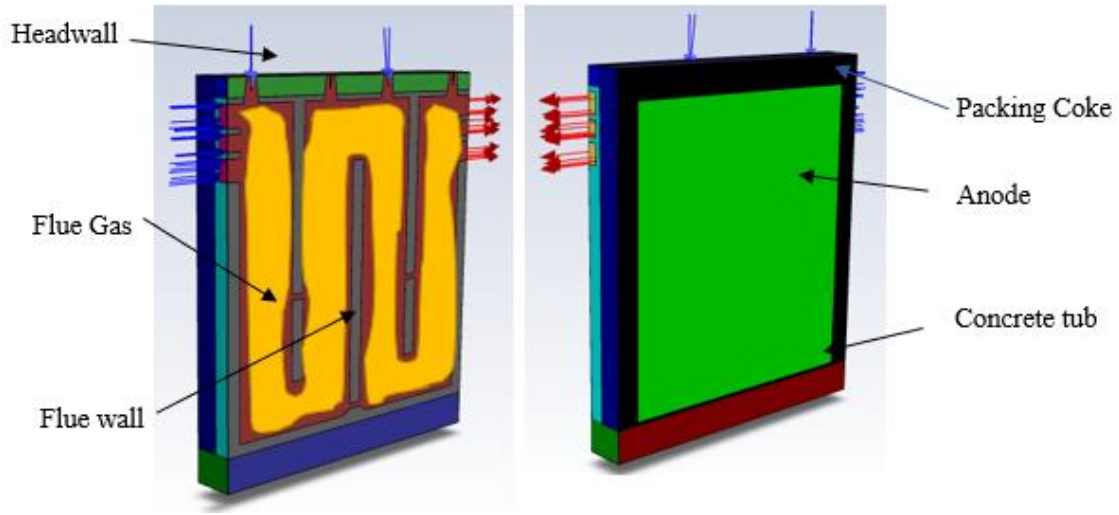

Figure 2. Schematic of computational domain.

2.1 Assumptions

- 100 % of pitch volatiles are getting combusted.
- Fuel is burned completely (100 % combustion efficiency).
- Packing coke bed is assumed to be a multi-dispersed particle system. Void fraction and specific surface area were calculated based on granulometry data. Thermal conductivity of packing coke bed was calculated as a function of void fraction and temperature, using correlation given by Akito Kasai et al. [12].

$$k_{pc} = \{0.973 + (0.00634 * (T - 273))\} * (1 - \varepsilon^{2/3}) \quad (1)$$

where:
k_{pc} = Thermal conductivity of packing coke bed,
T=Temperature
ε = Void fraction of packing coke bed

- Perfect contact between solids (brick and packing coke, packing coke and anodes etc.) is assumed for heat conduction.
- Materials (brick, coke, anode etc.) are assumed to be isotropic in nature.
- Heat loss from top and bottom of the furnace is via convection and radiation mode.

All the anodes are assumed to be at uniform temperature at the beginning of preheating 1 section. Computed anode temperature for final time step of each section is considered as initial anode temperatures for the section next to them.

2.2 Governing Equations

Physical phenomena involved in baking process and mathematical equations solved to model them are tabulated in Table 2.

Table 2. Governing equations of model.

Physical Phenomena	Governing Equation
Mass conservation of flue gas	$\frac{\partial \rho}{\partial t} + \nabla \bullet (\rho U) = 0$ (2)
Momentum Conservation of flue gas	$\frac{\partial (\rho U)}{\partial t} + \nabla \bullet (\rho U \times U) = -\nabla P + \nabla \bullet \tau$ (3)
Turbulence in flow	k-ε turbulence equations: $\frac{\partial (\rho k)}{\partial t} + \nabla \bullet (\rho U.k) = \nabla.\left[\left(\mu + \frac{\mu_t}{\sigma_k}\right)\nabla \mathrm{k}\right] + P_k + P_{kb} - \rho\varepsilon$ (4) $\frac{\partial (\rho \varepsilon)}{\partial t} + \nabla \bullet (\rho U.\varepsilon) = \nabla.\left[\left(\mu + \frac{\mu_t}{\sigma_\varepsilon}\right)\nabla \varepsilon\right] + \frac{\varepsilon}{k}\left(C_{\varepsilon 1}(P_k + P_{\varepsilon b})\right) - C_{\varepsilon 2}\rho\varepsilon$ (5)
Energy Conservation	$\frac{\partial (\rho h_{tot})}{\partial t} - \frac{\partial P}{\partial t} + \nabla \bullet (\rho U h_{tot}) = \nabla.\left(\lambda_{ef} \nabla \bullet T_g\right) + \nabla \bullet (U.\tau) + S_E$ (6) $\lambda_{ef} = \lambda + \frac{C_p \mu_t}{P_{rt}}$ (7)
Heat transfer in solid through conduction	$\rho_s C_p \frac{dT_s}{dt} = \lambda_s \nabla \bullet T_s - Q_s$ (8)

Nomenclature:

P Density of flue gas (kg/m^3)
U Flue gas Velocity (m/s)
T Time (s)
τ Shear Stress Tensor
h_{tot} Specific total enthalpy of flue gas (J/kg)
P Flue gas pressure (Pa)
T_s Solid Temperature (ºC)
S_E Energy Source (W/m^3)
λ Thermal conductivity (W/mK)
λ_{ef} Effective thermal conductivity (W/mK)
k Turbulence kinetic energy per unit mass (m^2/s^2)
ε Turbulence dissipation rate (m^2/s^3)
μ Molecular dynamic viscosity (kg/m s)
μ_t Turbulent viscosity (kg/m s)
σ_k, σ_ε, $C_{\varepsilon 1}C_{\varepsilon 2}$ Constants for k-ε turbulence model
P_k, P_{kb}, P_{eb} Shear production of turbulence
C_p Specific heat capacity of solid (J/kg K)
ρ_s Density of solids (kg/m^3)
Q_s Thermal loss to the atmosphere (W/m^3)
P_{rt} Turbulent Prandtl Number

2.3 Boundary Conditions

Flue gas inlet and outlet:

Due to changes in flue gas temperature, viscosity and density changes along the length and width of the furnace This leads to variation in volumetric flow rates and pressure drop across various sections. To take this effect into consideration, pressure drop across a fire (Preheating 1 to Zero pressure section) was measured. Mass flow rates of flue gas in individual sections were calculated through iterations, based on measured pressure drop values. As these mass flow rate values are calculated from measured pressure drop values, it takes care of air ingression phenomena. Section wise measured pressure drop values and calculated mass flow rate values are given in Figure 3.

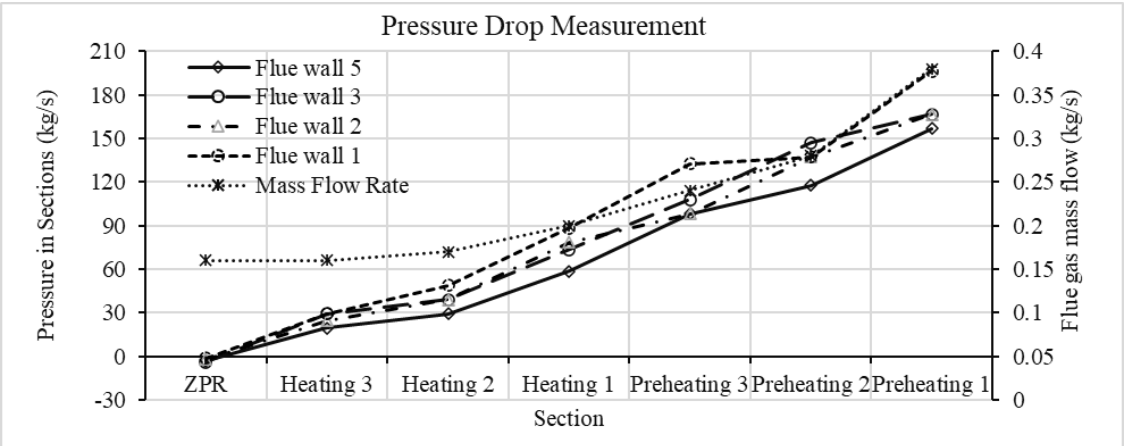

Figure 3. Pressure and mass flow rates in various sections of fire.

Heat loss:

Heat loss from ABF occurs through two ways:

- Convective and radiative heat loss from top surface of packing coke bed and head wall
- Heat lost to tub at the bottom of furnace

Convective and radiative heat transfer coefficients for top surfaces were calculated using correlations 7 and 8 given in ref [4].

$$h_{conv.} = 0.15\lambda\left(\frac{g.\beta}{\alpha.\nu}(T_s - T_\infty\right) \quad (7)$$

$$h_{rad.} = \sigma.\varepsilon.\left(\frac{T_s^4 - T_\infty^4}{T_s - T_\infty}\right) \quad (8)$$

Where:

h_{conv}. Convective heat transfer coefficient (W/m^{2}K)
h_{rad}. Radiative heat transfer coefficient (W/m^{2}K)
λ Thermal conductivity (W/mK)
α Thermal diffusivity (m^2/s)
ν Viscosity of air (kg/m s)
T_s Local surface temperature (K)
T_∞ Environment temperature (K)
σ Stephen Boltzmann constant
ε Thermal emissivity of surface
g Gravity (m/s^2)
β Thermal expansion coefficient

Environmental temperature is considered as 30 °C. Bottom of tub is cooled using forced air passing through the concrete pipe present beneath the tub of the ABF. Due to difficulty in measuring air flow rates and temperatures inside the cooling air pipe, heat transfer coefficient for bottom of furnace was calculated through iterations, based on measured bottom anode temperature.

Heat Source for pitch volatile combustion:

During a typical baking cycle, an anode loses its weight by 5 %. This baking loss can be equated to the mass of volatiles released in preheating zone. As per available literature, 1 ton of carbon anode releases 10 kg methane, 4 kg Hydrogen and 36 kg of tar [1]. Details of evolution temperature, ignition temperature, calorific values and combustion rates of these components are given in ref [5]. In this study, energy obtained from volatile combustion is calculated analytically and applied as heat source in flue gas volume as a function of anode temperature.

Light stock heavy Sulphur (LSHS) oil burning:

Average LSHS consumption per baking cycle for past one year was considered. Mass flow rate of combustion gases representing total combustion product was calculated. Equivalent quantity of hot gas was injected in flue gas channel as a stoichiometric mixture of CO_2 and H_2O. Inlet temperature of hot gas stream was calculated by equating heat released through combustion to the total enthalpy of injected gas, i.e.

$$\dot{m}_{LSHS}.CV_{LSHS} = \dot{m}_{hotgas}.h_{hotgas} \quad (9)$$

Where, $\dot{m}_{LSHS}$ and CV_{LSHS} are mass flow rate and calorific value of heavy fuel oil, respectively. $\dot{m}_{hotgas}$ and h_{hotgas} are mass flow rate and sensible enthalpy of hot gas, respectively. The mass flow rate and temperature of the hot gas were calculated as 0.0045 kg/sec per burner and 4100 °C, respectively (Similar approach is used by Francois G. *et al.*, who reported hot gas flow rate 0.0032 kg/sec per burner and temperature 3750 °C). These values were applied as boundary conditions at hot gas inlets. Symmetry (zero flux transfer) boundary conditions were applied at the center of the flue gas channel and center of pit. The equations were solved using finite volume method in ANSYS Fluent commercial code. To ensure convergence and accuracy of solution, timestep calculated using Courant number criteria was applied during initial 10 seconds of every simulation. Post this time, time-step of 1 sec was used. The residual convergence criteria were set to 10^{-3} for turbulence, velocity, and continuity solution. For energy equation, residual was set to 10^{-6}.

3. Plant Measurement

Measurement campaign was carried out with the objective of collecting anode baking profile data for model validation and studying impact of baking parameters on baked anode quality. To study variation in thermal profile across the width of section pits 1, 3, 5 and 9 were selected for thermal measurement. A batch of 28 green anodes was selected for experiments. Anodes were numbered and critical green anode quality parameters such as green anode density, height, width, and weight of anodes etc. were recorded. Green anodes were loaded in such a pattern that they were placed in 7th column of loading pattern. At the time of anode loading, thermocouples were placed adjacent to seventh column of anodes. Position of thermocouple probes in the pit is shown in figure 2. N type thermocouples with temperature range of -10 to 1200 °C and accuracy ± 5 °C were selected for the temperature measurement. Data logger HIKOI LR8431-20, was used for recording temperature data for the baking cycle. Data logger settings, such as type of thermocouple, temperature measurement range, data recording interval and measurement cycle time etc., were configured. Cycle time of 18 days with measurement interval of 5 min was selected. Data logger and thermocouples were connected with N type lead wire. These wires were protected by using a C-shaped cover. To provide continuous power supply to data recorder unit, electric extension board with Earth leakage circuit breaker (ELCB) was provided. Whole setup is shown in Figure 4 (a, b, and c).

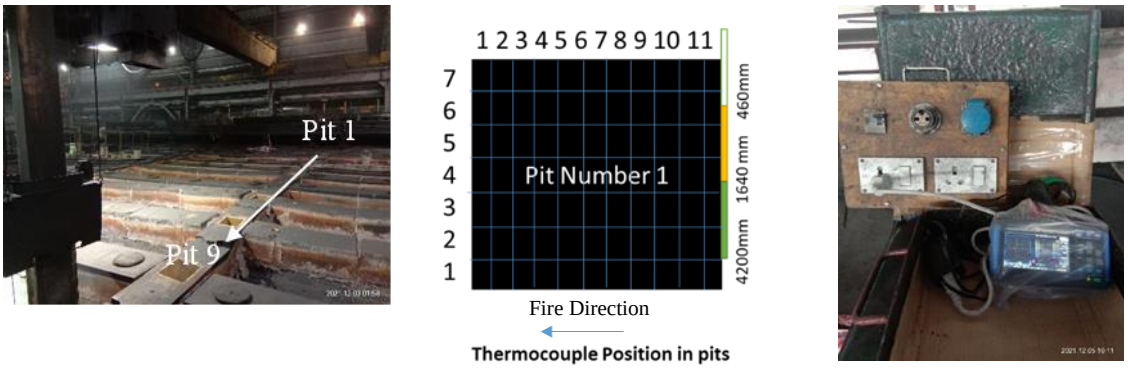

(a) (b) (c)

Figure 4. (a) Section selected for measurement (b) Position of thermocouples in pit (c) Data logger with ELCB.

Core-drill samples from 28 anode specimen loaded in 7th column of pit 1,3,5 and 9 were extracted and tested in laboratory. Correlation analysis was performed to study impact of thermal evolution faced by anode on its properties.

4. Results and Discussion

4.1 Model Validation

Model was simulated for preheating, heating, and cooling sections of anode baking furnace. Computed anode temperature at the time of end of these sections were compared against the measured temperatures of anodes at three points located at different heights of the pit. Figure 5 shows computed anode temperature contour with comparison of measured and computed anode temperatures in the mid-plane of anode.

The comparison of measured and computed anode temperatures shows a good agreement between model results and plant data. 2 % error was observed in computed anode temperature at 4600 mm depth in pit. This deviation can be attributed to the use of hot gas jet approach used for model fuel burning in heating zone. In their comparative study of combustion modelling approaches, Francois G. *et al*, have mentioned the need of calibrating the velocity of the hot gas jets to ensure more realistic heating of bottom of flue wall and other solids in ABF [9]. This calibration work was done by the authors to further improve the accuracy of model. 3.6 % error was observed in computed anode temperature at 460 mm. Computed anode temperature at bottom of pit are lower as compared to temperature of anode in top layer. However, measured anode temperatures in bottom of the furnace were found higher as compared to temperature of anodes in top layer. This can also be related to under heating of solids in bottom layer of furnace due to lower depth of hot gas jet as compared to depth of flames computed through combustion models. Measured baking profiles for location 1,2 and 3 in pit 1,3,5 and 9 are shown in Figure 6. Baking parameter data obtained from these curves is summarized in Table 3.

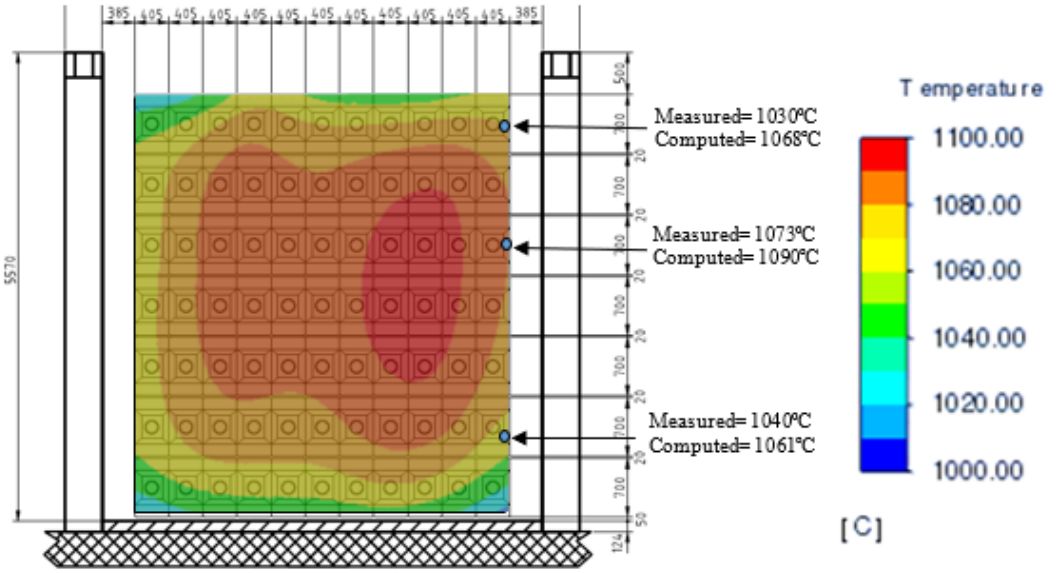

Figure 5. Predicted anode temperature contour at midplane of pit and predictive accuracy in % with measured temperature data.

Table 3. Baking parameters seen by anodes in top, middle and bottom layer of pit

Layer No	Maximum Baking temperature (°C)	Time spent above 1000 °C (hours)
7	1 035	34
4	1 073	94.5
2	1 041	62

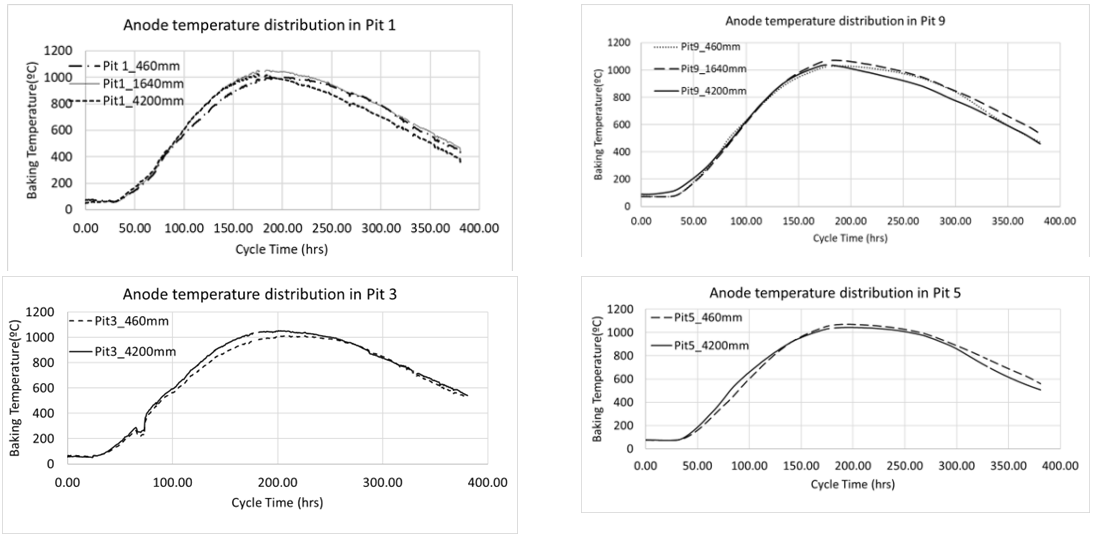

Figure 6. Measured baking profiles at various locations in pits of ABF.

From baking curve measurement data and simulation results, it was observed that middle layer of anodes is reaching maximum temperature. Whereas top and bottom layer of anodes is not reaching the expected baking temperature. Gas flow distribution computed using the model shows low velocity regimes in region near to the top layer of anodes and bottom corners of the pit. To study the impact of these non-homogenous temperature distribution on anode quality, layer wise samples were analysed in laboratory. Anode layers were numbered according to sequence of loading of green anodes in the pit. Layer 7 is the top layer and layer 1 is the bottom layer of anodes. Property variations across the height of the pit has been presented in Figure 7.

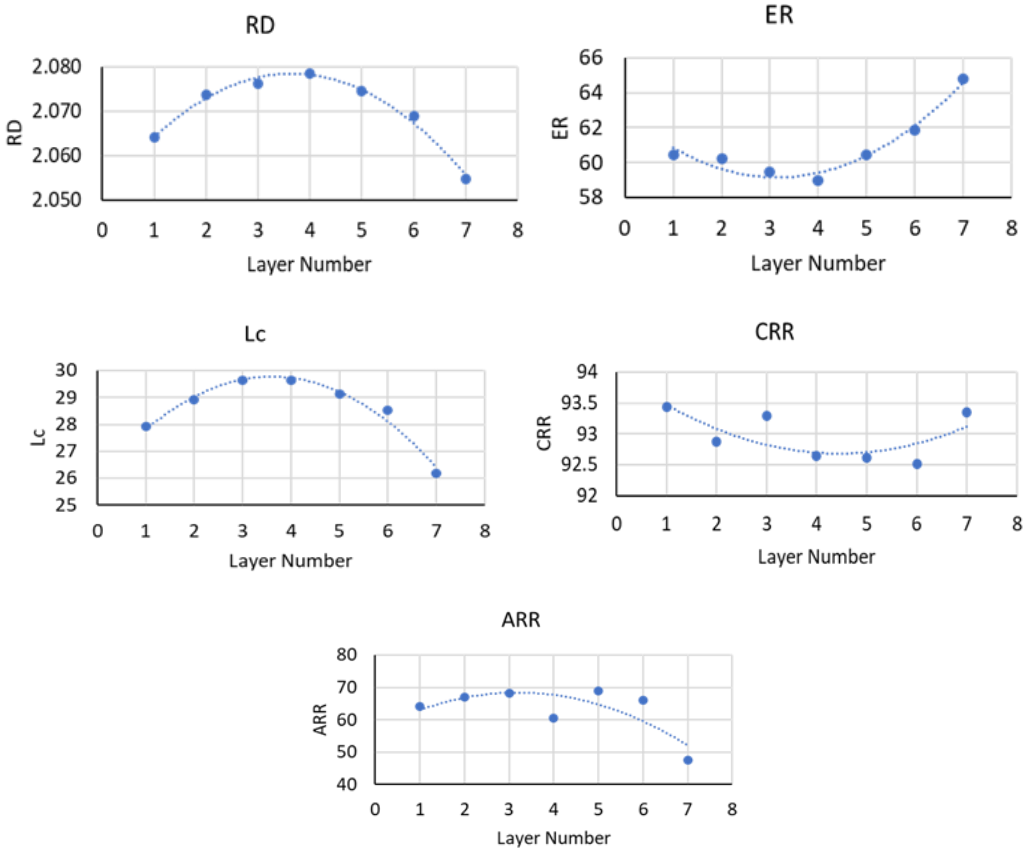

Figure 7. Baked anode properties of anode samples collected from various layers

Impact of variation in baking temperature and soaking time (time above 1000 °C) seen by anodes located at various heights in pit was reflected in final properties of anode samples. Variation in RD across the layers in pit is observed. Maximum RD was obtained in layer 4 and minimum RD was obtained in top layer. Indicates strong positive correlation with maximum baking temperature attained during fire. Lc for anodes in all layers remained in lower than usual range due to subpar baking parameters observed during fire. Maximum Lc value (29.8) was achieved in 3rd and 4th layer where greatest value of maximum baking temperature was reached. Desulphurization in carbon anodes increases with increase in baking temperature. Desulphurization leads to increase in air permeability and surface area within the anode [10]. This creates additional sites for Carbon-CO_2 reaction during electrolysis in pots. Hence, minimum Carboxy reaction residue (CRR) observed in anode placed in 4th layer can be correlated to the maximum baking temperature observed during fire. ER of prebaked carbon anodes is reported as a function of coke granulometry, sulfur content of coke, pitch content in green mix and baking parameters [11]. However, in current study strong correlation was observed between ER and baking parameters. Minimum ER value (58.8) was achieved in 4th layer where greatest value of maximum baking temperature (1073 °C) was reached. This can be attributed to high RD and Lc obtained for these anodes. Air reactivity residue (ARR) of carbon anodes is a function of differential reactivity of coke-binder matrix and content of inorganic catalysts such as Sodium and Vanadium [10,11]. In present case, ARR was found to be in range of 49 % to 69 % which is relatively low as compared to industry standard of 72-80 %. Low ARR is indicative of subpar baking, high standard deviation observed in ARR of anode samples points towards non-homogeneous temperature distribution inside the pit.

5. Conclusion

- To identify reasons behind high ER, low ARR and cracking of anodes in pot, detailed study of plant process was performed, and baking was identified as the most influential cause.
- To analyse the performance of anode baking process, a computational model was developed. Measurement campaign was carried out to study thermal evolution of anodes at various heights of pits during a baking cycle.
- Computational results were validated against the measured data. Accuracy of predicted results was found to be in range of 93 % to 98 %. Which is acceptable for industrial furnaces.
- Computed as well as measured anode temperature data show non-homogeneity in baking across height and length of the pit. This non-homogeneity strongly impacts anode quality parameters like ER and Lc. Anodes in middle layer see maximum temperature and spends most amount of time above 1000 °C. Whereas anodes in top layer and bottom layer were not able to reach the desired baking temperature. As a result, quality of anodes was found to be degrading in order: middle layer, bottom layer, and top layer. Based on these findings, authors have initiated a study to improve overall baking efficiency and temperature homogeneity inside furnace. Process parameters and flue wall design is being optimized through CFD analysis, onsite experiments, and trials. Details of this study will be communicated through another paper.

6. References

1. Felix Keller, Peter O. Sulger, *Baking of Anodes for the Aluminium Industry*, 2nd Edition, Sierre, R&D Carbon, 2008, 559 pages.
2. Roy A Cahill, Patrice Palau, Common root causes for anode problems within the reduction cell, *12th Australasian Aluminium Smelting Technology Conference,* 2018, Queenstown, New Zealand, 1-20.

3. Werner K. Fischer, Felix Keller, Baking parameters and the resulting anode quality, *Light Metals* 1993, 427-435.
4. Theodore L. Bergman et al, *Fundamentals of Heat and Mass Transfer*, 8th Edition, Wiley, December 2018.
5. E. Dernedde et al., Kinetic phenomena of the volatiles in ring furnaces, *Light Metals* 1986, 589-592.
6. Dagoberto S. Severo, Vanderlei Gusberti, Elton C. V. Pinto, Advanced 3D modelling for anode baking furnaces, *Light Metals* 2005, 697-702.
7. Felix Keller et al., Specific energy consumption in anode baking furnaces, *Light Metals* 2010, 408-413.
8. Mounir Baiteche et al., Description and applications of 3d mathematical model for horizontal anode baking furnace, *Light Metals* 2015, 1115-1120.
9. Francois Gregoire, Louis Gosselin, Comparison of three combustion models for simulating anode baking furnaces, *International Journal of Thermal Sciences*, Vol. 129, (2018), 532-544.
10. Khalil Khaji, Mohammed Al Qassemi, Factors influencing baked anode properties, *Light Metals* 2015, 1135-1140.
11. Werner K. Fischer et al., Baking parameters and resulting anode quality, *Light Metals* 1993, 427-433.
12. Akito Kasai et al., Measurement of effective thermal conductivity of coke, *ISIJ International*, vol 33. (1993), 697-702.